PHYSICSAccess Research Paper
ISSN Online: 2756-3898, ISSN Print: 2714-500X https://doi.org/10.47514/phyaccess.2026.6.2.019

Integrated Instrumentation System for Extracellular Electrophysiological Signal Acquisition in Amaranthus

Ndung'u R Wairimu[1], Riara Martin[1], Fidelis Ngugi[1], and Kamweru P Kuria[2]

[1] Department of Basic Sciences, Tharaka University, Nairobi, Kenya
[2] Department of Physical Sciences, Chuka University, Nairobi, Kenya

Corresponding E-mail: ruthwairimu237@gmail.com

Received 24-09-2026
Accepted for publication 06-11-2026
Published 12-11-2026

Abstract

Plant extracellular electrical signals are low-amplitude and susceptible to interference from the electrode–plant interface, recording electronics, and the surrounding environment. This study describes the development of an instrumentation system for recording extracellular electrical potentials in Amaranthus. The redesigned system incorporated an AD620 instrumentation amplifier, modified Ag/AgCl electrodes, an Anfatec USBLockIn 250 lock-in amplifier, and electromagnetic shielding. Although the lock-in amplifier was included in the signal-acquisition chain, synchronous detection of plant electrical signals could not be independently verified because no modulation or excitation mechanism was documented in the archived experimental records. Recordings were obtained from five plants subjected to alternating six-hour irrigation-withheld and post-irrigation periods over three consecutive days. The initial LF356N prototype and redesigned configuration were compared descriptively using the recorded mean, standard deviation (SD), signal dynamic range (SDR), normalized voltage range (NVR), and relative variability (RV). NVR decreased from 1.0367 to 0.1216, and RV decreased from 0.2992 to 0.0356. In contrast, SDR increased from 10.813 to 10.900 mV, while SD increased from 3.120 to 3.189 mV. The mean recorded potential shifted from −10.430 to 89.663 mV. Since NVR and RV are normalized by the absolute mean, their lower values do not independently demonstrate reduced electronic noise, improved accuracy, or increased sensitivity. Furthermore, the configurations were not independently calibrated or compared using known electrical inputs, and the available records do not establish matched test conditions. The irrigation-withheld and post-irrigation observations represent repeated measurements from the same five plants rather than independent biological replicates. Soil moisture and plant water status were also not measured. Overall, the findings are descriptive and highlight the need for further electrical and biological characterization of the instrumentation system.

Keywords: Plant electrophysiology; extracellular electrical potential; instrumentation amplifier; Ag/AgCl electrodes; signal conditioning; irrigation withholding.

 ©DOP_KASU Publishing

I. Introduction

Plants continuously perceive and respond to environmental stimuli through coordinated chemical, hydraulic, mechanical, and electrical signalling pathways [1–3]. Among these mechanisms, electrical signalling provides a rapid means of transmitting information between different regions of a plant and contributes to systemic responses to environmental changes [4–7]. Plant bioelectrical signals arise primarily from the movement of ions across cellular membranes through specialized ion channels and transporters. The movement of potassium (K^+), calcium (Ca^{2+}), chloride (Cl^-), and protons (H^+) generates transient changes in membrane potential that propagate through conductive tissues, particularly the phloem [8–10]. Depending on the initiating stimulus, these responses occur as action potentials (APs), variation potentials (VPs), or system potentials (SPs), each exhibiting distinct propagation characteristics and physiological functions [9], [13]. These signalling mechanisms have attracted increasing interest in plant biology, biophysics, biosensing, and applications involving plant monitoring and stress responses [11–12].

The measurement of plant extracellular electrical signals, however, presents significant instrumentation challenges [14–15]. Recorded signals may occur at microvolt-to-millivolt levels, while plant tissues exhibit relatively high electrical impedance. The electrode–plant interface introduces additional sources of measurement variability, including polarization potentials, electrode offsets, changes in contact impedance, and baseline drift [16–17]. Environmental electromagnetic interference and mechanical movement can further obscure low-amplitude biological signals and reduce recording stability [18]. Since extracellular measurements represent voltage differences between recording and reference electrodes, electrode position, tissue characteristics, contact conditions, and reference stability are important determinants of the recorded waveform [15], [19].

Several approaches have consequently been investigated to improve plant electrophysiological signal acquisition. These include instrumentation amplifiers such as the AD620, which provide high input impedance and common-mode rejection, as well as Ag/AgCl and other electrode configurations designed to improve electrical contact and reduce polarization effects [20]. Signal-conditioning techniques, including analogue filtering, differential amplification, lock-in amplification, adaptive filtering, and digital denoising, have also been applied to improve the extraction of weak electrical signals in noisy environments [21]. More recent developments include flexible sensors and organic electrochemical transistor-based devices, which offer improved mechanical compliance and alternative approaches to interfacing with plant tissues [11], [22].

Despite these advances, challenges remain in integrating the electrode interface, analogue front-end, amplification, filtering, and interference-reduction stages into a stable signal-acquisition system. Improvements in individual components do not necessarily compensate for signal degradation introduced elsewhere in the measurement chain [23–24]. Electrode polarization, impedance variation, electromagnetic interference, motion artefacts, baseline instability, and low signal-to-noise ratio can collectively affect the reproducibility of extracellular recordings. An integrated instrumentation approach that considers the electrode interface, amplification, signal conditioning, and interference reduction as components of a unified acquisition architecture is therefore warranted.

This study focused on the design and descriptive evaluation of an integrated instrumentation system for extracellular electrical-potential acquisition in Amaranthus. The system combined modified Ag/AgCl electrodes, an AD620 instrumentation amplifier, analogue signal conditioning, a lock-in amplifier stage, and electromagnetic shielding. Although the lock-in amplifier was part of the connected hardware pathway, the available records do not establish whether synchronous detection of plant electrical signals occurred during the experiments. Recorded voltage characteristics from the redesigned configuration were compared descriptively with those from an initial LF356N-based prototype. This comparison was not a calibrated, controlled head-to-head assessment, as the electrode interface and electronic stages were changed together, and independent measurements of gain, frequency response, and noise were unavailable. In addition, the irrigation-withholding experiment was used to describe the temporal voltage variations in five plants during irrigation-withheld and post-irrigation periods, rather than to establish a validated measure of plant water status.

II. Materials and Methods

The instrumentation system was developed in two stages. The first involved the fabrication and testing of an initial prototype for acquiring extracellular electrical potentials from Amaranthus. The second involved redesigning the amplifier and electrode interface and incorporating additional signal-conditioning and shielding components. The recorded voltage characteristics of the two configurations were compared descriptively. Since independent calibration and matched-input testing were not performed, the comparison was not interpreted as definitive evidence of improved instrument performance.

A. Prototype Instrument Design

The initial prototype comprised an LF356N operational amplifier and passive components, including 10 kΩ and 100 kΩ resistors and a 1 µF capacitor, arranged in a circuit for acquiring extracellular electrical potentials from Amaranthus. The circuit was assembled on a breadboard, powered by a 15 V DC supply, and configured as a voltage follower. The circuit configuration and fabrication stages are shown in Fig. 1.

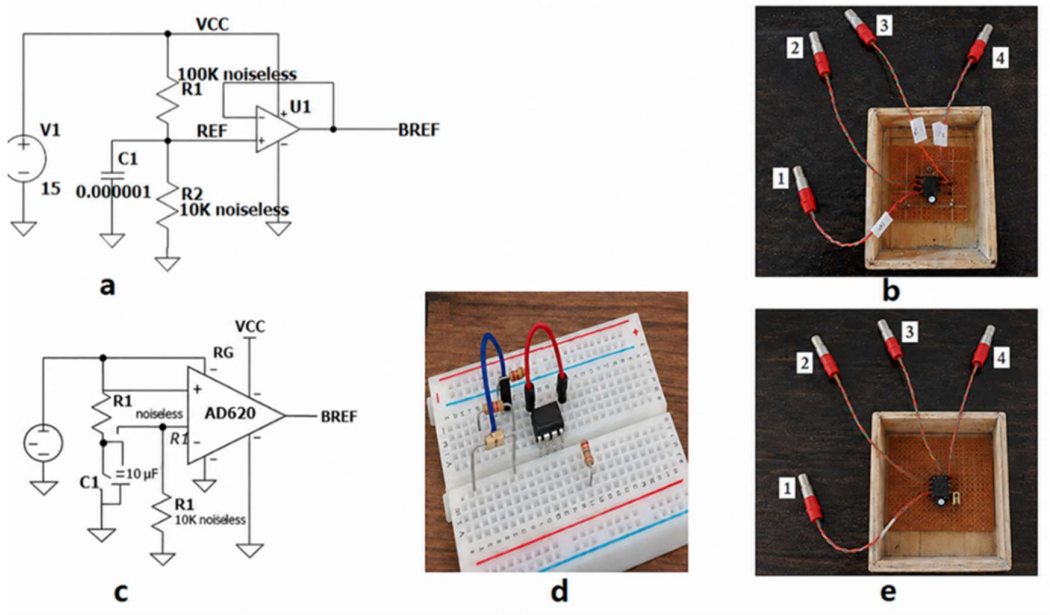


Fig. 1. Development of the plant electrophysiological signal acquisition system: (a) Initial circuit diagram; (b) Initial designed and fabricated kit; (c) Improved schematic diagram of the amplifier; (d) Breadboard prototype; and (e) Final assembled prototype.

Plant–electrode coupling in the initial prototype was achieved using custom-made Ag/AgCl electrodes fabricated from chlorinated silver wire (99.99% purity, 0.5 mm diameter). The wire was chlorinated by anodisation in 0.1 M KCl within a stainless-steel needle containing 3 M KCl solution. The amplifier assembly used four external leads: lead 1 was connected to the 15 V DC supply, lead 3 served as the reference connection, lead 4 received the plant signal, and lead 2 carried the amplifier output to the subsequent acquisition equipment. The electrode arrangements used in the initial and improved prototypes are shown in Fig. 2.

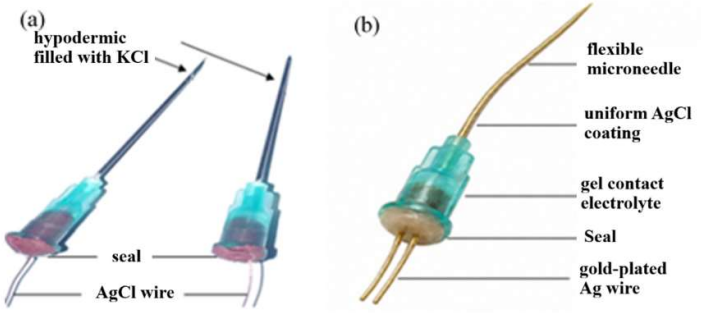


Fig. 2. Initial (a) and improved (b) microelectrodes.

B. Improved Instrument Design

The redesigned acquisition system comprised an electrode interface, differential amplification, analogue signal conditioning, a lock-in amplifier, an oscilloscope/data-acquisition interface, and computer-based data logging. Table I summarises the components and operating parameters documented in the experimental records. Where operating details were unavailable or could not be verified, this is explicitly indicated rather than inferred.

The recorded signal path was as follows: Ag/AgCl recording and reference electrodes → AD620 instrumentation amplifier → capacitive coupling stage → Anfatec USBLockIn250 lock-in amplifier → oscilloscope/data-acquisition interface → computer for data storage and analysis.

The inclusion of the lock-in amplifier in this pathway indicates only that the device was connected as part of the hardware arrangement. The archived experimental records do not document a modulation or excitation stage that would translate the low-frequency biological signals to the lock-in reference frequency. Consequently, although the lock-in amplifier formed part of the connected instrumentation chain, synchronous signal recovery and any associated improvement in signal-to-noise ratio could not be verified.

Table I: Instrumentation Components and Documented Operating Parameters.

Stage	Parameter	Value	Model/Component	Reason / Justification
Electrode System	Recording electrode	Stem, ~5 cm above root-stem junction	Flexible Ag/AgCl microneedle electrode	Stem placement ~5 cm above the root–stem junction; position maintained during each recording.
	Reference electrode	Leaf surface	Flexible Ag/AgCl microneedle electrode	Leaf-region reference electrode; exact contact site maintained during each recording.
	Contact medium	1–2% agar, 1 M KCl	Agar-KCl electrolyte gel	Improves ionic coupling, lowers interface impedance, and reduces motion artefacts.
Amplifier	Instrumentation amplifier	Nominal Gain = 50.4 V/V	AD620	Calculated from the 1 kΩ gain-setting resistor and the AD620 gain equation; assembled-system gain was not measured. AD620 bandwidth in the assembled circuit was not documented or measured
	Gain-setting resistor (R_G)	1 kΩ	Precision metal-film resistor	Produces gain of approximately 50.4 according to the AD620 gain equation.
Reference Bias Circuit	Voltage divider R_1	100 kΩ	Metal-film resistor	Establishes stable reference potential with minimal current draw.
	Voltage divider R_1	10 kΩ	Metal-film resistor	Generates a reference voltage of approximately 1.36 V.
	Filter capacitor (C_1)	1 µF	Electrolytic capacitor	1 µF is the value recorded for the reference/bias capacitor C1; its in-circuit effect was not independently characterized.
Power Supply	Positive supply rail	+15 V	DC laboratory power supply	Provides adequate headroom for low-noise analog amplification. The negative supply connection (AD620 pin 4) and the complete supply configuration were not documented.
Signal Conditioning	Coupling capacitor (C_C)	1 µF (nominal; unverified)	Electrolytic capacitor	Nominal value of 1 µF as recorded in the design documentation. The capacitance actually installed could not be verified from the available experimental records, so this value and the associated filter characteristics (including the high-pass corner it would define) are treated as unverified and are shown with a dashed outline in Fig. 3 and 4.
Lock-in Detection	Lock-in amplifier model	Anfatec USBLockIn250; 10 kHz reference	Two-phase digital lock-in amplifier	The device was present within the connected signal-acquisition pathway. However, the experimental records did not document the modulation source, reference signal generation, input configuration, sensitivity, time constant, filter slope, or output settings required to verify synchronous detection. Consequently, the functional contribution of the lock-in amplifier could not be established retrospectively. The 10 kHz reference value is as listed in the records; its source was not documented.
Data Acquisition	Sampling rate	1 sample/s	DAQ/Oscilloscope	Digital recording rate (one sample per second); distinct from the 10 kHz lock-in reference and analogue filter response.
	Software	Microsoft Excel	PC data logging platform	Used for storage, processing and calculation of NVR, RV and SDR metrics.

Fig. 3 illustrates the AD620 front-end and signal-conditioning pathway, while Fig. 4 presents the overall signal-acquisition chain. In both figures, solid outlines indicate parameters documented in the archived experimental records, whereas dashed amber outlines marked "not documented" or "unverified" identify parameters that could not be confirmed.

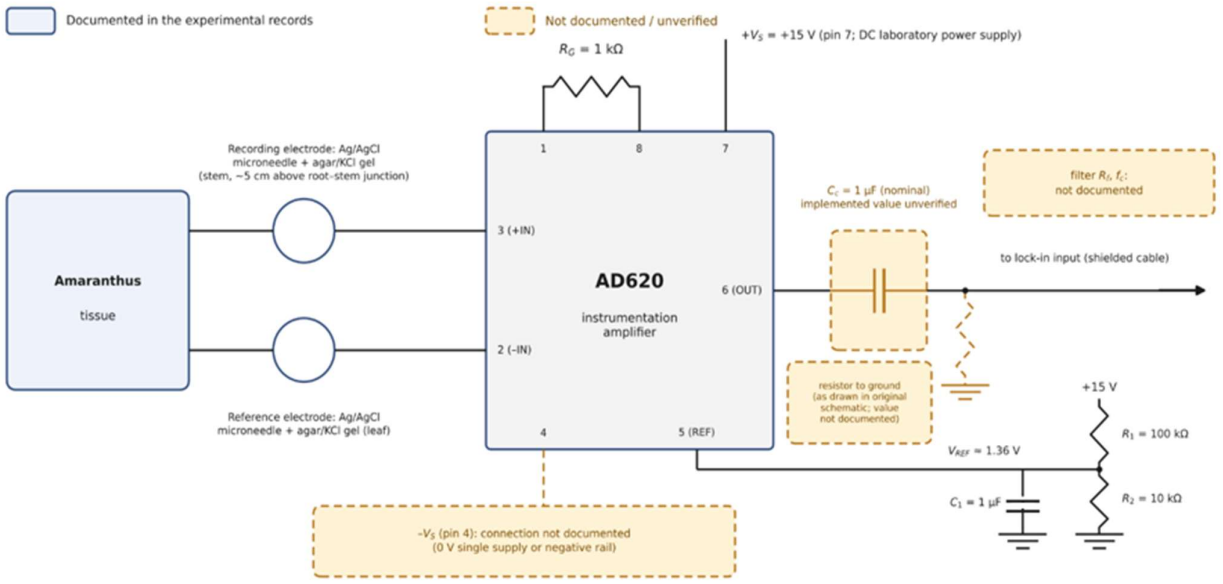


Fig. 3. Conceptual AD620 front-end and signal-conditioning pathway reconstructed from the available records. Solid outlines: documented parameters. Dashed amber outlines: not documented or unverified (coupling capacitor, filter characteristics, negative supply connection; see Table I).

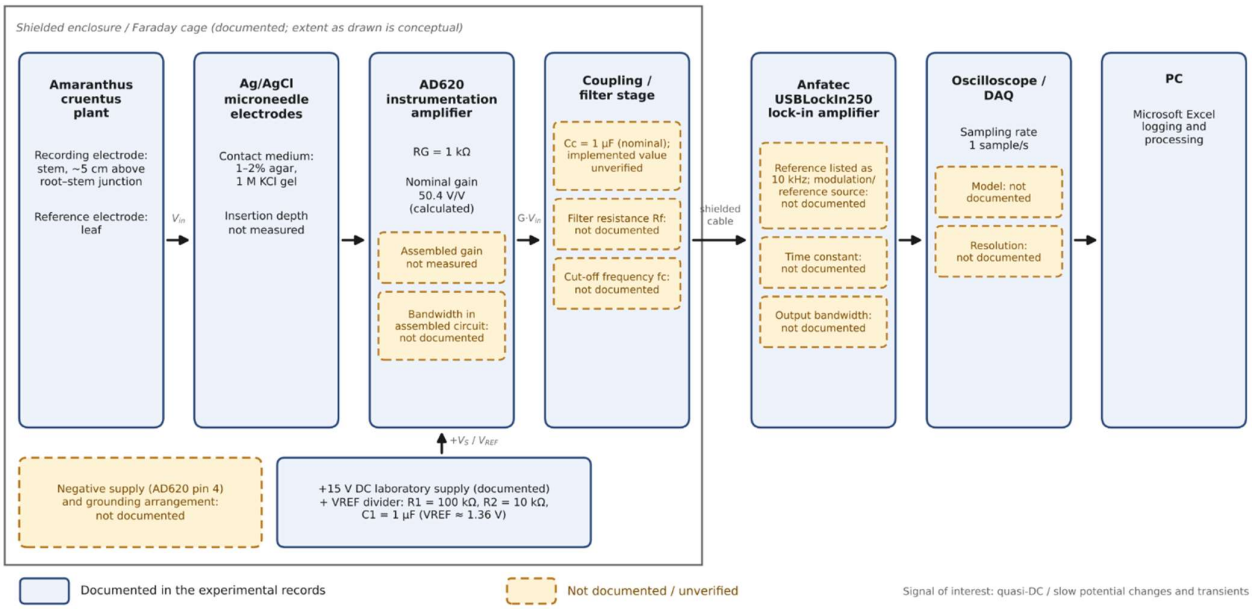


Fig. 4. Conceptual signal-acquisition chain reconstructed from the available experimental records. Solid outlines indicate documented parameters; dashed amber outlines indicate parameters that are not documented or could not be verified (see Table I).

The Ag/AgCl microneedle electrodes were connected to the AD620 instrumentation amplifier within a shielded enclosure. The amplified signal passed through a coupling stage and shielded cable to the lock-in amplifier, followed by oscilloscope/data-acquisition and computer-based recording. The AD620 nominal gain of 50.4 V/V was calculated from the recorded 1 kΩ gain-setting resistor; the gain of the assembled system was not measured. The records also document a $+15\,V$ supply rail, a reference-voltage divider comprising $R_1 = 100\,k\Omega$ and $R_2 = 10\,k\Omega$, a reference voltage of approximately 1.36 V, a 1 µF capacitor C_1, and a digital sampling rate of 1 sample/s.

However, the negative supply connection of the AD620 (pin 4), grounding arrangement, assembled-circuit bandwidth,

filter resistance and cut-off frequency, lock-in time constant, output bandwidth, modulation/reference source, and oscilloscope/DAQ model and resolution were not documented. The $1\,\mu F$ coupling capacitor is therefore identified as unverified because its installed value could not be confirmed (Table I). These parameters are marked as undocumented rather than assigned assumed values. Accordingly, the figures should not be interpreted as a complete characterisation of the assembled circuit.

The redesigned architecture incorporated differential amplification, a modified electrode interface, analogue coupling and filtering, and electromagnetic shielding. The AD620 was selected as the instrumentation amplifier, with its nominal gain calculated using a 1 kΩ external gain-setting resistor. This represents a component-based design value rather than an experimentally verified gain for the assembled system.

The AD620 gain is given by (1).

$$G = 1 + \frac{49.4\ k\Omega}{R_G} \quad (1)$$

where G is the nominal voltage gain (V/V) and R_G is the external gain-setting resistance. For $R_G = 1\ k\Omega$, the calculated gain is approximately $50.4\ V/V$.

The redesigned electrode interface used flexible Ag/AgCl microneedle electrodes with gold-plated flexible shafts and a gel contact medium comprising 1–2% agar with 1 M KCl. The recording electrode was positioned on the stem, approximately 5 cm above the root–stem junction, while the reference electrode was attached to the leaf region. These positions were maintained throughout each recording session. The microneedles were inserted sufficiently to establish electrical contact; however, the insertion depth was not quantitatively measured.

C. *Plant Material and Experimental Procedure*

The redesigned instrumentation system was used to record extracellular electrical potentials from Amaranthus cruentus plants subjected to alternating irrigation-withheld and post-irrigation periods. The plants were grown individually in 15 × 15 cm plastic containers filled with a mixture of soil and organic manure at the Tharaka University farm greenhouse. At the beginning of the recording period, the plants were approximately four weeks old.

The plants were maintained under natural lighting conditions, with a photoperiod of approximately 10–12 hours and a reported greenhouse temperature range of 25–30 °C. They were watered daily, except during the defined irrigation-withholding periods. Five plants served as biological experimental units, with repeated recordings obtained from the same plants during the irrigation-withheld and post-irrigation periods.

The measurement arrangement is shown in Fig. 5. Recordings were conducted inside a Faraday cage (Fig. 6) to reduce electromagnetic coupling from the surrounding laboratory environment. Although the cage provided electromagnetic shielding, it did not replace independent characterisation of electronic noise in the acquisition system.

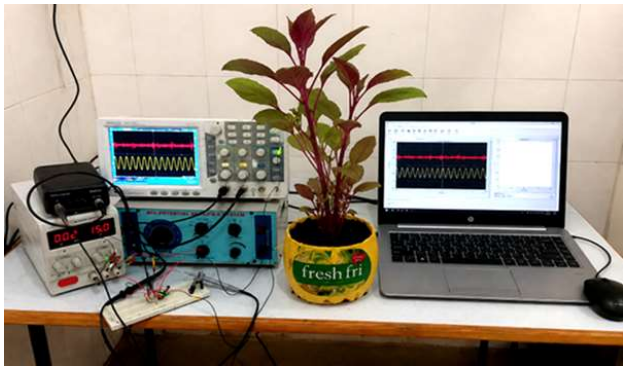


Fig. 5. Electrical potential measurement instrumentation showing the transmission of plant signals to the detection system.



Fig. 6. Electrical potential measurement setup with the Amaranthus plant inside a Faraday cage.

The experimental treatments consisted of a six-hour period during which irrigation was withheld, followed by irrigation and a subsequent six-hour post-irrigation period. One irrigation-withholding/post-irrigation cycle was conducted daily for three consecutive days. Soil moisture was not monitored during the experiment, and no direct measurements of soil-water content or plant-water status were obtained. Consequently, no soil-moisture monitoring procedure, measurement instrument, or quantitative soil-water threshold can be reported.

The terms "dry" and "wet" are therefore used operationally to refer to the irrigation-withholding and post-irrigation periods, respectively, and should not be interpreted as measured soil-moisture conditions. In Fig. 7–9 and Table II, "dry" (D) denotes the irrigation-withheld period, while "wet" (W) denotes the post-irrigation period. Electrical potentials were recorded repeatedly from the same five plants during these scheduled periods. These repeated observations do not constitute independent biological replicates.

Electrical potentials were monitored during the alternating six-hour irrigation-withheld and six-hour post-irrigation periods over three consecutive days. The acquisition system recorded at a rate of 1 sample/s, and the resulting data were stored for subsequent analysis. This digital recording rate is

distinct from the lock-in reference frequency and the analogue filter cut-off frequency.

Before each recording period, the instrumentation system was allowed to reach a stable operating condition. Initial transients associated with switching on the system and establishing electrode–plant contact were observed before measurements were retained. However, the duration and numerical criterion for stabilisation were not documented.

D. Signal Analysis

Three descriptive quantities were calculated from the recorded voltage traces: Normalized Voltage Range (NVR), Relative Variability (RV), and Signal Dynamic Range (SDR). Since NVR and RV are normalised by the absolute mean voltage, they describe relative voltage excursion and dispersion, respectively, rather than directly measuring electronic noise, accuracy, or sensitivity. These quantities were interpreted alongside the voltage–time traces.

The Normalized Voltage Range (NVR) was calculated using (2).

$$NVR = \frac{V_{max} - V_{min}}{|\bar{V}|} \quad (2)$$

where V is the recorded voltage (mV), V_{max} and V_{min} are the maximum and minimum recorded voltages (mV), respectively, and $\bar{V}$ is the mean recorded voltage (mV) over the same recording interval. The denominator, $|\bar{V}|$, represents the absolute value of the mean. NVR is dimensionless and expresses the peak-to-peak voltage excursion relative to the absolute mean recorded voltage. It is sensitive to changes in the mean baseline.

NVR is a descriptive normalised range statistic. A lower value indicates a smaller observed peak-to-peak range relative to the absolute mean; it does not, by itself, demonstrate reduced electronic noise or improved instrument performance.

Relative Variability (RV) was calculated using (3).

$$RV = \frac{\sigma V}{|\bar{V}|} \quad (3)$$

where σV is the standard deviation of the recorded voltage (mV), and $|\bar{V}|$ is the absolute mean recorded voltage (mV). RV is dimensionless and represents the relative dispersion of the recorded voltage values. It is not an independently measured electronic-noise parameter.

Signal Dynamic Range (SDR) was determined using (4):

$$SDR = V_{max} - V_{min} \quad (4)$$

where V_{max} and V_{min} are the maximum and minimum recorded voltages (mV), respectively, over the same recording interval. SDR represents the peak-to-peak voltage range and is expressed in millivolts.

The three quantities were evaluated alongside the voltage–time traces. SDR describes the measured peak-to-peak excursion, whereas NVR and RV express the voltage range and standard deviation, respectively, relative to the absolute mean. No independent noise-floor measurement, known-input calibration, gain verification, or frequency-response measurement was performed. The analysis is therefore descriptive.

III. Results and Discussion

A. Descriptive Comparison of the Prototype and Redesigned Instrumentation Configurations

The initial LF356N-based prototype was used to acquire extracellular voltage recordings from Amaranthus plants. This configuration comprised a breadboard circuit and rigid stainless-steel needle electrodes containing KCl solution. The recorded voltage traces exhibited baseline variation and were susceptible to changes in electrode contact and movement artefacts. These observations describe the recorded signals; the study did not separately quantify the contributions of electronic noise, electrode polarisation, or environmental interference.

The instrumentation platform was subsequently redesigned using an AD620 instrumentation amplifier, flexible Ag/AgCl microneedle electrodes, gel contact, analogue signal conditioning and a printed circuit board (PCB) assembly housed within a shielded enclosure. These modifications were intended to provide a more integrated acquisition arrangement. However, because several components were changed simultaneously and no controlled component-by-component comparison was conducted, the effect of any individual modification cannot be isolated.

The AD620 has component-level characteristics suitable for differential signal amplification, including high input impedance and high common-mode rejection under specified operating conditions [25]. In this study, a 1 kΩ gain resistor gave a calculated nominal gain of approximately 50.4 V/V. However, the gain and frequency response of the assembled system were not independently measured. Thus, the component specifications provide the design rationale but do not constitute verified performance measurements of the complete instrument.

The redesigned electrode configuration replaced the rigid needle electrodes and liquid KCl contact used in the initial prototype with flexible microneedle electrodes and an agar–KCl gel contact medium. This arrangement was introduced to provide a more compliant electrode–plant interface and potentially maintain physical contact during recording. Nevertheless, contact impedance, electrode polarisation, long-term drift and motion artefacts were not independently measured. The redesigned electrode arrangement is therefore described as a design modification intended to facilitate electrode–plant contact, rather than as a demonstrated improvement in recording fidelity.

The Anfatec USBLockIn250 was incorporated downstream of the signal-conditioning stage. The archived records confirm its physical presence in the acquisition pathway but do not establish that lock-in signal recovery was successfully implemented. Since no modulation or excitation mechanism was documented, the effectiveness of synchronous detection could not be evaluated retrospectively. Accordingly, the lock-in amplifier is reported as part of the connected hardware configuration, not as a verified source of signal enhancement.

B. Temporal Electrical Responses of Amaranthus during Irrigation-withheld and Post-irrigation Periods

The temporal extracellular potential profiles recorded from Amaranthus during the alternating irrigation-withheld and post-irrigation periods are presented in Fig. 7. The figure shows a selected segment of the archived record rather than the complete three-day series. The recorded voltage varied over time within the plotted segment. Changes are visible during the intervals labelled dry (irrigation-withheld) and wet (post-irrigation). However, because soil moisture and plant water status were not measured, these variations are reported as observations associated with the irrigation schedule and cannot be attributed directly to soil-water availability.

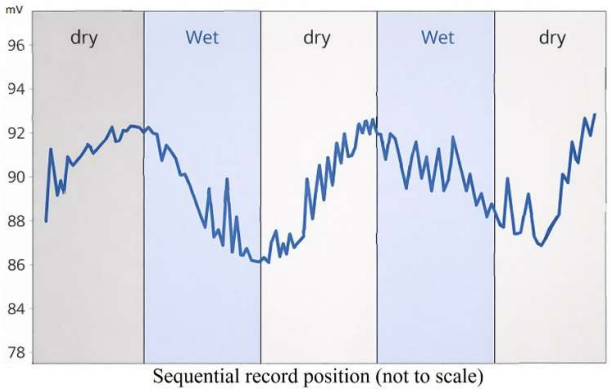


Fig. 7. Recorded extracellular potential trace for a selected segment of the archived record, not the complete three-day series. Shaded intervals are labelled "dry" (irrigation-withheld) and "wet" (post-irrigation). The horizontal axis indicates sequential position within the plotted segment only and does not represent elapsed time.

Fig. 7 contains five consecutive shaded intervals: three labelled dry (irrigation-withheld) and two labelled wet (post-irrigation). The Methods section describes one six-hour irrigation-withheld period followed by one six-hour post-irrigation period on each of three consecutive days, giving six scheduled intervals in total. Fig. 7 therefore presents only a selected segment and does not show the complete experimental sequence.

The archived plot contained an inconsistent horizontal time axis, including a duplicated "1080 min" label. Consequently, the intervals cannot be mapped unambiguously onto the documented schedule. The original time-series data and acquisition log are unavailable, so the segment's day, cycle, and original timestamps cannot be established. To avoid implying unsupported elapsed times, the numerical time labels have been removed, and the horizontal axis is presented as sequential record position (not to scale). Fig. 7 should therefore be interpreted as an illustration of the available recorded segment, rather than as a quantitative timeline of the three-day experiment.

Within the plotted segment, the recorded potential generally increased during some irrigation-withheld intervals and decreased during post-irrigation intervals. This pattern is descriptive and does not establish a plant physiological response, a specific mechanism, or an effect of water availability. Membrane potential, ion fluxes, and plant water status were not measured concurrently. Although previous studies have reported changes in plant electrical activity under water-related treatments [6], [27], the present measurements do not establish that the same mechanisms produced the observed voltage variations.

Repeated voltage changes were observed in the same five plants during the monitoring period. These observations demonstrate temporal variation within the experimental plants but do not establish independent biological reproducibility. Furthermore, the records do not demonstrate the absence of baseline drift or random noise, as these quantities were not independently characterised. Accordingly, the data do not establish instrument sensitivity, measurement stability, or reliable discrimination of plant water status.

C. Mean Electrical Potential during Irrigation-withheld and Post-irrigation Periods

Fig. 8 presents the mean recorded electrical potentials for the scheduled irrigation-withheld and post-irrigation periods over the three-day experiment. On Day 1, the reported means were approximately 90.4 mV for the post-irrigation period and 89.8 mV for the irrigation-withheld period. These values are descriptive summaries of the recorded data.

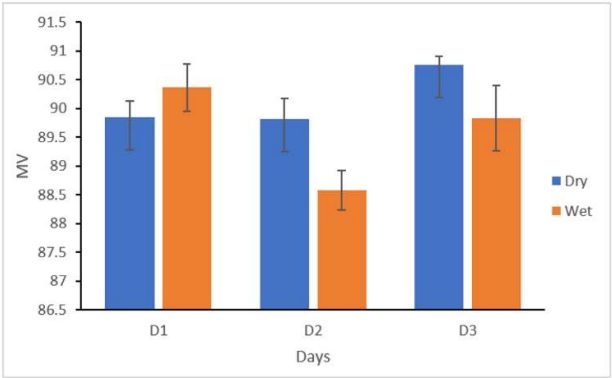


Fig. 8. Mean electrical potential (EP) of Amaranthus during irrigation-withheld (Dry) and post-irrigation (Wet) periods on each of the three days (D1–D3).

The recorded mean potentials differed across the scheduled periods. On Day 2, the mean potential during the post-irrigation period decreased to 88.6 mV, whereas the irrigation-withheld mean remained at 89.8 mV. On Day 3, the highest reported mean, 90.8 mV, occurred during the irrigation-withheld period. The post-irrigation mean increased slightly to 89.8 mV but remained below the irrigation-withheld mean. These values describe the recorded observations only; soil moisture and plant water status were not measured.

The observed differences cannot be attributed directly to water availability or a specific physiological process. The

experiment used operationally defined irrigation-withheld and post-irrigation periods without measuring soil-water content or plant water status. Further work combining electrical recordings with direct measurements of water status and independent plant replicates is needed to determine whether the observed voltage differences are consistently associated with the irrigation schedule.

The reported standard deviations and distributions describe variability in the recorded observations. Since measurements were obtained repeatedly from the same five plants, individual time points do not constitute independent biological replicates. No mixed-effects model or other inferential statistical test was performed. Therefore, statistical significance cannot be inferred from visual differences or error bars.

The differences between the mean recorded potentials during the irrigation-withheld and post-irrigation periods varied in magnitude and direction across the three days. These differences are insufficient to demonstrate instrument sensitivity or reliable discrimination between the periods. Establishing such properties would require calibrated electrical inputs, independent noise characterisation, quantified plant water status, additional independent plants, and an analysis that accounts for repeated measurements.

D. Distribution of Electrical Potential Measurements

Fig. 9 shows the distributions of the recorded electrical potential (EP) values for the irrigation-withheld (D) and post-irrigation (W) periods on each of the three days. The box plots present the median, interquartile range (IQR), overall spread, and potential outliers of repeated measurements from the five plants.

On Day 1, the two distributions overlapped considerably. On Day 2, the irrigation-withheld period showed a higher median. On Day 3, the medians were similar, while the spread was markedly narrower during the irrigation-withheld period, which also appears to contain fewer plotted observations. The IQR differed between the two periods on each day. These differences describe the recorded measurements only. Since soil moisture and plant water status were not measured, and repeated observations from the same five plants are not independent biological replicates, the distributions do not establish a physiological response or an effect of water availability. Investigating such a relationship would require independent plants and concurrent measurements of plant water status.

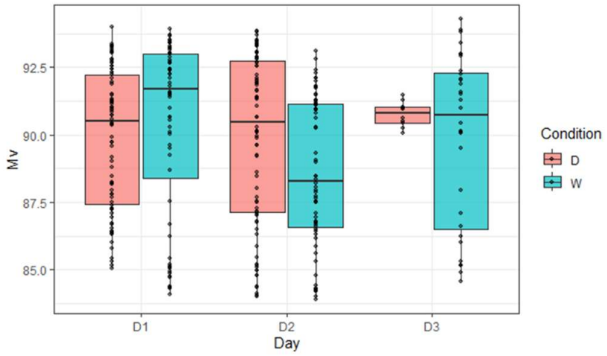


Fig. 9. Distribution of the electrical potential (EP) of Amaranthus during irrigation-withheld (D) and post-irrigation (W) periods on each day (D1–D3).

E. *Descriptive Evaluation of Recorded Voltage Characteristics*

The initial and redesigned configurations were compared using the recorded mean voltage, standard deviation (SD), Signal Dynamic Range (SDR), Normalized Voltage Range (NVR), and Relative Variability (RV). These quantities describe the recorded voltage distributions. Table II presents the numerical comparison. Since the mean baseline shifted substantially and the configurations were not independently calibrated under matched, known-input conditions, the normalised differences cannot be interpreted as evidence of improved accuracy, reduced electronic noise, or enhanced sensitivity.

Table II: Descriptive Comparison of Recorded Voltage Characteristics.

Metric	Initial Prototype	Redesigned Configuration	Change	Redesigned System (Irrigation-withheld)	Redesigned System (Post-irrigation)
Mean Potential (mV)	-10.430	89.663	+100.093 mV	89.965	89.341
SD (mV)	3.120	3.189	+2.21 %	2.985	3.372
SDR (mV)	10.813	10.900	+0.80 %	10.800	10.813
NVR	1.0367	0.1216	-88.27 %	0.1200	0.1210
RV	0.2992	0.0356	-88.10 %	0.0332	0.0378

Fig. 8 presents the daily mean electrical potentials separately for the irrigation-withheld and post-irrigation periods on Days 1–3. In contrast, the values in Table II were calculated from the pooled recorded observations within each respective dataset. The mean of 89.663 mV represents the overall redesigned-configuration dataset, whereas 89.965 mV and 89.341 mV represent the pooled irrigation-withheld and post-irrigation datasets, respectively. These values are not arithmetic averages of the daily means shown in Fig. 8. Because the Table II statistics were calculated from the underlying observations rather than the three daily summary values, they need not equal averages calculated directly from Fig. 8. The pooled values are descriptive summaries of

repeated recordings from the same five plants and do not represent independent biological replicates.

The exact number of observations contributing to each pooled dataset could not be verified retrospectively from the archived records. The datasets therefore represent repeated measurements from the same five plants and do not constitute independent biological replicates.

The SD increased from 3.120 mV in the initial prototype to 3.189 mV in the redesigned configuration. SDR changed from 10.813 to 10.900 mV, an increase of approximately 0.80%. The mean recorded voltage shifted from −10.430 to 89.663 mV, a difference of 100.093 mV. This substantial baseline shift affects the normalised quantities and may reflect differences in the electrode interface, reference configuration, amplification, signal conditioning, grounding, or other changes between the configurations. The available records do not allow these contributions to be separated.

For the redesigned configuration, the mean recorded potential was 89.965 mV during the scheduled irrigation-withheld period and 89.341 mV during the scheduled post-irrigation period. The corresponding SD values were 2.985 and 3.372 mV, SDR values were 10.800 and 10.813 mV, NVR values were 0.1200 and 0.1210, and RV values were 0.0332 and 0.0378, respectively. The difference between the means was 0.624 mV. These descriptive differences do not establish reliable discrimination between plant-water-status conditions.

NVR decreased from 1.0367 to 0.1216, while RV decreased from 0.2992 to 0.0356. However, both metrics are normalised by the absolute mean voltage, which changed from 10.430 to 89.663 mV. The absolute SD did not decrease, and the SDR remained similar. The lower normalised values therefore indicate a lower voltage range and dispersion relative to the magnitude of the recorded mean; they do not demonstrate reduced electronic noise, improved measurement accuracy, or increased sensitivity. Furthermore, the configurations differed in several hardware and electrode features, and the comparison was neither independently calibrated nor conducted using a documented matched electrical input.

The numerical comparison is descriptive and does not establish that the redesigned instrument outperformed the initial prototype in accuracy, sensitivity, or noise performance. Rather, it documents differences in the recorded voltage distributions that require follow-up testing using known electrical inputs, gain and frequency-response measurements, and independent noise characterisation.

F. Synthesis and Interpretation of the Overall Findings

Taken together, the results show that both configurations produced extracellular voltage recordings from Amaranthus and that the recorded voltage distributions differed. The comparison is descriptive because the electrode interface, amplifier, and signal-conditioning pathway were changed together; the mean voltage shifted substantially; and independent calibration, matched-input comparison, and direct noise measurements were not performed. The lower NVR and RV values indicate lower normalised variability in the recorded data, not a demonstrated reduction in electronic noise or improvement in measurement accuracy. The time-series recordings obtained during the irrigation-withheld and post-irrigation periods show temporal variation within five plants, but the respective contributions of plant physiology, electrode contact, and the acquisition chain cannot be separated.

Previous studies have described instrumentation approaches for plant electrophysiology, including multichannel low-noise recording, configurable acquisition systems and integrated amplifier/electrode arrangements [28]. These studies provide context for the design choices considered in the present work. However, the contribution of each component was not independently tested, and the study did not establish that the lock-in stage improved the signal-to-noise ratio. The results should therefore be interpreted as a description of the assembled acquisition configuration rather than evidence of a quantified systems-level performance gain.

The recordings showed temporal and distributional variation during the scheduled irrigation-withheld and post-irrigation periods. Previous studies have reported plant electrical changes associated with water-related treatments [29–30], but soil moisture and plant water status were not measured concurrently in the present study. The small difference between the irrigation-withheld and post-irrigation mean values (0.624 mV), considered in relation to the observed variability, does not establish reliable classification of the two conditions. The recorded changes cannot be assigned to a specific physiological mechanism or used to validate extracellular potential as a standalone indicator of plant water status.

The experiment used five Amaranthus plants as biological experimental units, with repeated electrical-potential measurements obtained from each plant over successive irrigation-withheld/post-irrigation cycles. The individual time points are repeated observations, not additional independent plants. No mixed-effects model was fitted, and no inferential statistical results are reported. In addition, the fixed sequence of irrigation withholding followed by irrigation introduces temporal confounding. Further studies should use more independent plants, randomized or counterbalanced treatment sequences where feasible, and statistical methods that account for repeated observations.

A further limitation of the available experimental records concerns the operation of the lock-in amplifier. Although an Anfatec USBLockIn250 was incorporated into the acquisition chain, the records do not document a modulation source or synchronous reference pathway. Consequently, it was not possible to determine whether synchronous detection contributed to the recorded measurements. The lock-in amplifier is therefore reported as part of the hardware architecture rather than as a demonstrated signal-processing operation.

Overall, this study documents the construction of an integrated acquisition arrangement and its use in recording extracellular voltage variations in Amaranthus. The recorded metrics provide descriptive information about the voltage distributions but do not establish measurement accuracy, sensitivity, reduced electronic noise, or validated discrimination between treatment periods. Further work is required to calibrate the complete signal chain, characterise its frequency response and noise, document lock-in operation, and measure plant water status concurrently with electrical potential. Table III summarises the observations, what the data support and what they do not establish.

Table III: Summary of observations and interpretation.

Aspect	Recorded observation	What the data support	What the data do not establish	Further work required
Prototype comparison	Mean: −10.430 → 89.663 mV; SD: 3.120 → 3.189 mV; SDR: 10.813 → 10.900 mV.	The recorded voltage distributions differed between configurations.	Accuracy, sensitivity, reduced electronic noise, or the causal effect of a single component.	Known-input calibration and matched-condition comparison.
Normalized metrics	NVR: 1.0367 → 0.1216; RV: 0.2992 → 0.0356.	Lower range and dispersion relative to the absolute mean voltage.	Direct electronic-noise reduction or improved measurement quality.	Independent noise-floor and transfer-function measurements.
Irrigation-withheld vs post-irrigation comparison	Mean: 89.965 mV (irrigation-withheld) and 89.341 mV (post-irrigation); difference 0.624 mV.	A small descriptive difference in recorded means.	Reliable discrimination or validated measurement of plant water status.	Concurrent soil-moisture and plant-water-status measurements.
Experimental units	Five plants measured repeatedly over three days.	Temporal observations within five biological experimental units.	Independent replication from each time point or inferential statistical significance.	More independent plants and repeated-measures analysis.

IV. Materials and Methods

An instrumentation system for recording extracellular electrical potentials in Amaranthus was developed, progressing from an LF356N-based prototype to a redesigned configuration incorporating an AD620 amplifier, flexible Ag/AgCl microneedle electrodes, gel contact, analogue signal conditioning and electromagnetic shielding. Although an Anfatec USBLockIn250 was included in the acquisition chain, successful synchronous detection could not be verified from the available records.

The mean recorded voltage shifted from −10.430 mV to 89.663 mV between the initial and redesigned configurations. Although NVR and RV decreased, the absolute SD increased slightly from 3.120 to 3.189 mV, while SDR remained nearly unchanged. These results do not establish reduced electronic noise, improved accuracy, or increased sensitivity, particularly in the absence of independent calibration using known electrical inputs.

Recordings from five plants showed temporal variations during irrigation-withheld and post-irrigation periods, with a pooled mean difference of 0.624 mV. However, this difference does not establish reliable discrimination of plant water status, as soil moisture and plant water status were not measured, and repeated observations do not constitute independent biological replicates. Overall, the study demonstrates the use of the assembled system to record extracellular voltage variations but does not establish calibrated performance or a specific physiological origin of the signals.

Future work should focus on calibrating and characterising the complete instrumentation system, independently evaluating its noise and frequency response, and verifying lock-in operation. Biological validation should involve more independent plants and concurrent measurements of soil moisture and plant water status under different stress conditions. Standardised recording protocols and appropriate repeated-measures analysis will also be necessary to establish reproducibility and assess the potential of the system for plant monitoring.

References

[1] E. D. Brenner, R. Stahlberg, S. Mancuso, J. Vivanco, F. Baluška, and E. Van Volkenburgh, "Plant neurobiology: An integrated view of plant signaling," *Trends Plant Sci.*, vol. 11, no. 8, pp. 413–419, 2006, doi: 10.1016/j.tplants.2006.06.009.

[2] A. E. Huber and T. L. Bauerle, "Long-distance plant signaling pathways in response to multiple stressors: The gap in knowledge," *J. Exp. Bot.*, vol. 67, no. 7, pp. 2063–2079, 2016, doi: 10.1093/jxb/erw099.

[3] A. Novoplansky, G. M. Souza, E. D. Brenner, S. C. Bhatla, and E. Van Volkenburgh, "Exploring the complex information processes underlying plant behavior," *Plant Signal. Behav.*, vol. 19, no. 1, Art.

no. 2411913, 2024, doi: 10.1080/15592324.2024.2411913.
[4] W.-G. Choi, G. Miller, I. Wallace, J. Harper, R. Mittler, and S. Gilroy, "Orchestrating rapid long-distance signaling in plants with Ca^{2+}, ROS and electrical signals," *Plant J.*, vol. 90, no. 4, pp. 698–707, 2017, doi: 10.1111/tpj.13492.
[5] W.-G. Choi, R. Hilleary, S. J. Swanson, S.-H. Kim, and S. Gilroy, "Rapid, long-distance electrical and calcium signaling in plants," *Annu. Rev. Plant Biol.*, vol. 67, pp. 287–307, 2016, doi: 10.1146/annurev-arplant-043015-112130.
[6] J. Fromm and S. Lautner, "Electrical signals and their physiological significance in plants," *Plant Cell Environ.*, vol. 30, no. 3, pp. 249–257, 2007, doi: 10.1111/j.1365-3040.2006.01614.x.
[7] A. Gallé, S. Lautner, J. Flexas, and J. Fromm, "Environmental stimuli and physiological responses: The current view on electrical signalling," *Environ. Exp. Bot.*, vol. 114, pp. 15–21, 2015, doi: 10.1016/j.envexpbot.2014.06.013.
[8] M. Klejchova, F. A. Silva-Alvim, M. R. Blatt, and J. C. Alvim, "Membrane voltage as a dynamic platform for spatiotemporal signaling, physiological, and developmental regulation," *Plant Physiol.*, vol. 185, no. 4, pp. 1523–1541, 2021, doi: 10.1093/plphys/kiab032.
[9] M. Szechyńska-Hebda, M. Lewandowska, and S. Karpiński, "Electrical signaling, photosynthesis and systemic acquired acclimation," *Front. Physiol.*, vol. 8, Art. no. 684, 2017, doi: 10.3389/fphys.2017.00684.
[10] V. Vodeneev, L. Katicheva, and V. Sukhov, "Electrical signals in higher plants: Mechanisms of generation and propagation," *Biophysics*, vol. 61, no. 3, pp. 505–512, 2016, doi: 10.1134/S0006350916030209.
[11] S. Zhou, J. Zhou, Y. Pan, Q. Wu, and J. Ping, "Wearable electrochemical sensors for plant small-molecule detection," *Trends Plant Sci.*, vol. 29, no. 2, pp. 219–231, 2024, doi: 10.1016/j.tplants.2023.11.013.
[12] M. Shoaib, S. U. Khan, H. AbdelHameed, and A. Qahmash, "Plant stress detection using multimodal imaging and machine learning: From leaf spectra to smartphone applications," *Front. Plant Sci.*, vol. 16, Art. no. 1670593, 2026, doi: 10.3389/fpls.2025.1670593.
[13] M. R. Zimmermann and A. Mithöfer, "Electrical long-distance signaling in plants," in *Long-Distance Systemic Signaling and Communication in Plants*, F. Baluška, Ed. Heidelberg, Germany: Springer, 2013, pp. 291–308, doi: 10.1007/978-3-642-36470-9_15.
[14] Y. Liu, D. Li, J. Qian, B. Di, G. Zhang, and Z. Ren, "Electrical impedance spectroscopy (EIS) in plant roots research: A review," *Plant Methods*, vol. 17, Art. no. 118, 2021, doi: 10.1186/s13007-021-00817-3.
[15] D.-J. Zhao, Y. Chen, Z.-Y. Wang, L. Xue, T.-L. Mao, Y.-M. Liu, *et al.*, "High-resolution non-contact measurement of the electrical activity of plants in situ using optical recording," *Sci. Rep.*, vol. 5, Art. no. 13425, 2015, doi: 10.1038/srep13425.
[16] M. Weigand, F. M. Wagner, J. K. Limbrock, C. Hilbich, C. Hauck, and A. Kemna, "A monitoring system for spatiotemporal electrical self-potential measurements in cryospheric environments," *Geosci. Instrum. Methods Data Syst.*, vol. 9, no. 2, pp. 317–336, 2020, doi: 10.5194/gi-9-317-2020.
[17] S. Ha, C. Kim, Y. M. Chi, A. Akinin, C. Maier, A. Ueno, and G. Cauwenberghs, "Integrated circuits and electrode interfaces for noninvasive physiological monitoring," *IEEE Trans. Biomed. Eng.*, vol. 61, no. 5, pp. 1522–1537, 2014, doi: 10.1109/TBME.2014.2308552.
[18] T. Jochum, T. Denison, and P. Wolf, "Integrated circuit amplifiers for multi-electrode intracortical recording," *J. Neural Eng.*, vol. 6, no. 1, Art. no. 012001, 2009, doi: 10.1088/1741-2560/6/1/012001.
[19] D. R. Humphrey and E. M. Schmidt, "Extracellular single-unit recording methods," in *Neurophysiological Techniques: Applications to Neural Systems*, A. A. Boulton, G. B. Baker, and C. H. Vanderwolf, Eds., *Neuromethods*, vol. 15. Totowa, NJ, USA: Humana Press, 1990, pp. 1–64, doi: 10.1385/0-89603-185-3:1.
[20] C. Kitchin and L. Counts, *A Designer's Guide to Instrumentation Amplifiers*, 3rd ed. Norwood, MA, USA: Analog Devices, Inc., 2006.
[21] Y. Shi, H. Dou, A. Zhou, and Y. Chen, "Design and fabrication of a miniaturized electrochemical instrument and its preliminary evaluation," *Sens. Actuators B Chem.*, vol. 131, no. 2, pp. 516–524, 2008, doi: 10.1016/j.snb.2007.12.053.
[22] B. Xue, X. Su, L. Li, T. T. S. Lew, and C. Wu, "Wearable electrochemical bioelectronics for agriculture," *J. Mater. Chem. A*, vol. 12, no. 34, pp. 22396–22416, 2024, doi: 10.1039/D4TA02345E.
[23] J. P. Giraldo, H. Wu, G. M. Newkirk, and S. Kruss, "Nanobiotechnology approaches for engineering smart plant sensors," *Nat. Nanotechnol.*, vol. 14, no. 6, pp. 541–553, 2019, doi: 10.1038/s41565-019-0470-6.
[24] P. Coatsworth, L. Gonzalez-Macia, A. S. P. Collins, T. Bozkurt, and F. Güder, "Continuous monitoring of chemical signals in plants under stress," *Nat. Rev. Chem.*, vol. 7, no. 1, pp. 7–25, 2023, doi: 10.1038/s41570-022-00443-0.
[25] Analog Devices, Inc., "AD620: Low cost, low power instrumentation amplifier," Data Sheet. [Online]. Available: https://www.analog.com/media/en/technical-documentation/data-sheets/ad620.pdf.
[26] D. Tran, F. Dutoit, E. Najdenovska, N. Wallbridge, C. Plummer, M. Mazza, *et al.*, "Electrophysiological assessment of plant status outside a Faraday cage

using supervised machine learning," *Sci. Rep.*, vol. 9, Art. no. 17073, 2019, doi: 10.1038/s41598-019-53675-4.

[27] P. M. Gil, L. Gurovich, B. Schaffer, J. Alcayaga, S. Rey, and R. Iturriaga, "Root-to-leaf electrical signaling in avocado in response to light and soil water content," *J. Plant Physiol.*, vol. 165, no. 10, pp. 1070–1078, 2008, doi: 10.1016/j.jplph.2007.07.014.

[28] A. Armada-Moreira, C. Diacci, A. M. Dar, M. Berggren, D. T. Simon, and E. Stavrinidou, "Benchmarking organic electrochemical transistors for plant electrophysiology," *Front. Plant Sci.*, vol. 13, Art. no. 916120, 2022, doi: 10.3389/fpls.2022.916120.

[29] S. L. Chaparro-Cárdenas, J. A. Ramírez-Bautista, W. Gamboa-Contreras, A. L. Moreno-Chacón, and F. C. Vargas-Tangua, "Plant electrophysiology: Bibliometric analysis, methods and applications in the monitoring of plant-environment interactions," *DYNA*, vol. 88, no. 218, pp. 212–223, 2021, doi: 10.15446/dyna.v88n218.92405.

[30] N. Muramatsu and K. Hiraoka, "Water status detection of Satsuma mandarin (*Citrus unshiu* Marc.) trees using an electrical impedance method," *Environ. Control Biol.*, vol. 45, no. 1, pp. 1–7, 2007, doi: 10.2525/ecb.45.1.